AN INTEGRATED PLATFORM FOR CAVITY OPTOMECHANICS WITH VACUUM-SEALED SILICON PHOTONIC MEMS

Pierre Edinger[1,], Gaehun Jo[1], Simon J. Bleiker[1], Alain Y. Takabayashi[2], Niels Quack[2], Peter Verheyen[3], Umar Khan[3,4], Wim Bogaerts[3,4], Cleitus Antony[5], Frank Niklaus[1], and Kristinn B. Gylfason[1]*
[1]Division of Micro and Nanosystems, KTH Royal Institute of Technology, Stockholm, Sweden
[2]EPFL, Lausanne, Switzerland
[3]IMEC, Leuven, Belgium
[4]Ghent University, Gent, Belgium
[5]Tyndall National Institute, Cork, Ireland

ABSTRACT

Silicon photonics is an excellent platform for integrated cavity optomechanics due to silicon's high light confinement and favorable mechanical properties. However, optomechanical devices require a vacuum environment to inhibit damping due to air.

We present an integrated platform for cavity optomechanics using thermo-compression bonding of silicon caps to provide on-chip vacuum sealing. We demonstrate optomechanical coupling in a vacuum-sealed ring resonator implemented on the platform, either by modulation of the laser power or by using an electrostatic phase shifter in the ring.

By enabling optomechanics on a standard platform, we aim to make the technology available to a wider user base.

KEYWORDS

Silicon photonics, optomechanics, vacuum-sealing, silicon photonic foundry, silicon photonic MEMS.

INTRODUCTION

Cavity optomechanics, or the enhancement of the interaction between light and mechanical objects in resonant cavities, is an essential branch of physics with potential applications from quantum memories to high-precision sensing [1], [2]. Silicon photonics is a platform of choice for integrated optomechanics due to silicon's high light confinement and excellent mechanical properties [3]–[6].

However, integrated optomechanics requires dedicated fabrication steps for releasing movable structures and packaging steps for operation in vacuum. While the release of photonic Micro-Electro-Mechanical Systems (MEMS) [7] and optomechanical devices [8] has been demonstrated on chips and wafers from silicon photonic foundries, a platform with on-chip vacuum is not available yet. These challenges limit the development of the field to highly specialized labs and reduce the potential for commercialization.

Here, we present a platform for on-chip optomechanics, see Figure 1. The optomechanical devices are fabricated in a standard silicon photonic foundry process (IMEC's iSiPP50G), with a few post-processing steps to suspend the mechanical structures and seal the devices in a vacuum. The platform was originally developed for low-power programmable photonic chips using electrostatic MEMS actuators [7]. We demonstrate that the platform is well-suited for optomechanics using an optical add-drop ring resonator where the input and output directional couplers (DC) are connected to movable shuttles.

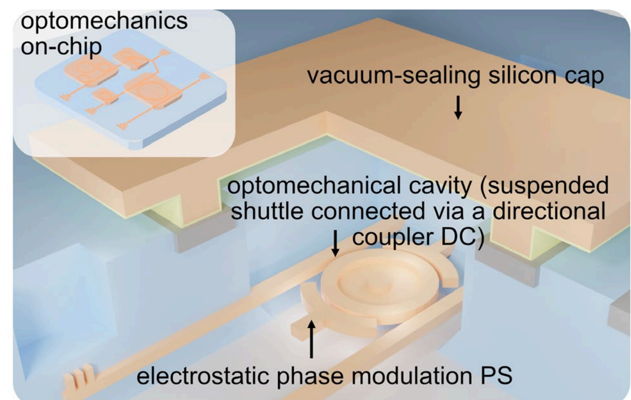

Figure 1: 3D sketch of the platform demonstrated in this paper for on-chip cavity optomechanics in silicon photonics. Silicon caps transferred using thermo-compression bonding provide local vacuum cavities for suspended photonic MEMS devices.

DESCRIPTION OF THE PLATFORM

The demonstrated platform for integrated cavity optomechanics comprises two main elements: optomechanical cavities with suspended movable structures and vacuum-sealing caps bonded above each device.

The demonstration device (Figure 2) consists of an add-drop photonic ring resonator (the optical resonant cavity), where the ring waveguide is mechanically anchored to a central silicon disk suspended on an oxide pillar; two movable waveguides attached to suspended DC shuttles; and two phase shifter shuttles (PS) controlling the optical round-trip length of the ring [9]. All four shuttles can be moved in-plane using electrostatic MEMS actuators or optomechanical coupling to the ring resonator cavity via the optical gradient force.

Authorized licensed use limited to: IMEC. Downloaded on June 02,2024 at 13:25:49 UTC from IEEE Xplore. Restrictions apply.

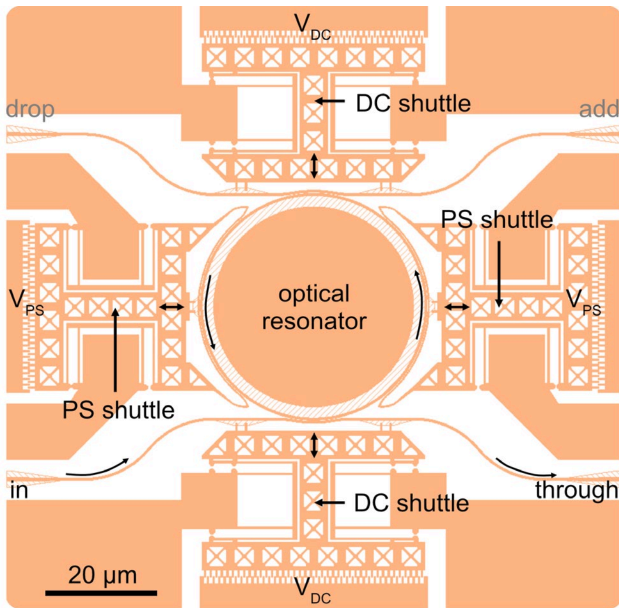

Figure 2: Layout of the photonic device used to demonstrate optomechanical coupling in our platform. The device consists of an add-drop ring resonator where electrostatic MEMS actuation can tune the input coupling, output coupling, and round-trip phase [9].

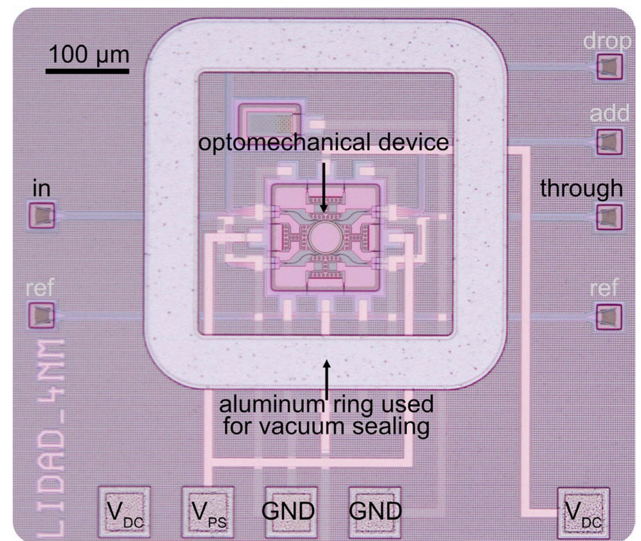

Figure 3: Microscope image of the fabricated device before vacuum-sealing. The ring resonator, waveguides, grating couplers, and electrical contacts were designed on a silicon photonic foundry platform (IMEC's iSiPP50G). The movable actuators were suspended using vHF etching of the buried oxide.

FABRICATION

The ring resonators were designed and patterned in a commercial 200 mm silicon photonic foundry platform (IMEC's iSiPP50G). The rings and the electrostatic MEMS actuators were suspended using vapor–phase Hydrogen Fluoride (vHF) acid etching (uEtch, SPTS) of the buried silicon dioxide layer on downsized 100 mm diameter wafers. Figure 3 presents the device after foundry fabrication and vHF release. For interfacing, the resonator is connected optically and electrically to grating couplers and bondpads, respectively, using standard designs from the foundry design kit. An aluminum ring defined on the same layer as the bondpads surrounds the released device to enable bonding of the sealing caps.

For the vacuum encapsulation of the optomechanical ring resonator, we first patterned and etched out the matching silicon caps on a 100 mm diameter silicon-on-insulator (SOI) wafer with a 25 µm thick device layer. Then, we bonded the SOI wafer containing silicon caps to the photonic foundry wafer by Al-Au thermo-compression bonding [10]. Finally, we etched away the handle layer of the SOI wafer with caps, and thus leaving the transferred individual vacuum-sealing caps on top of the resonators as illustrated in Figure 1. The use of individual sealing caps instead of a single chip-scale vacuum package provides local access to the grating couplers and electrical bondpads needed to interface the device.

MEASUREMENTS

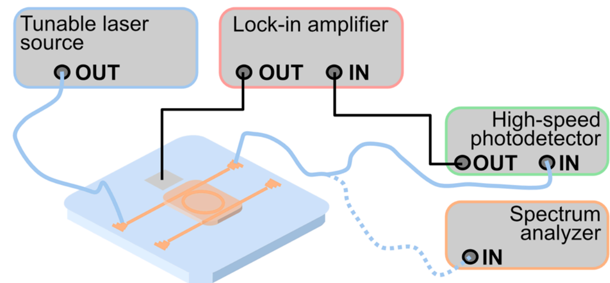

Figure 4: Sketch of the measurement setup. Depending on the measurement, we either used a spectrum analyzer or an high-speed photodetector connected to a lock-in amplifier as output.

Figure 4 presents the setup used for the different measurements. We used optical fibers aligned to grating couplers to couple light into and out of the chip. We used the transmission at the through port for all the measurements presented here. We used a tunable laser (Agilent 81680A) to set the wavelength and power and measured the transmission versus wavelength using a spectrum analyzer (Agilent 86082A). An example of a transmission measurement at the through port near a resonance is shown in Figure 5. The resonance exhibits an optical quality factor of 24,000 and an extinction ratio of over 15 dB. The two phase shifter shuttles can be moved in-plane using the electrostatic MEMS actuators to tune the round-trip phase of the ring resonator, resulting in a resonance shift. The response curve of the phase shifter is plotted in Figure 6(a).

Authorized licensed use limited to: IMEC. Downloaded on June 02,2024 at 13:25:49 UTC from IEEE Xplore. Restrictions apply.

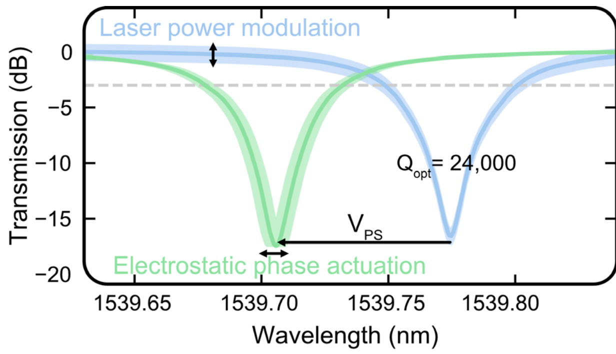

Figure 5: Optical transmission at the through port of the ring resonator near an optical resonance at 1539.75 nm, for two different phase shifter biases V_{PS}: 0 V (blue) and 10 V (green). The power can be modulated for the optomechanical experiments using the laser (wavelength-independent) or the phase shifter (wavelength-dependent).

The shuttles connected to the directional couplers can also be moved in-plane using electrostatic MEMS actuators. An offset bias V_{DC} can control the resonances' extinction ratio, as demonstrated in [9]. However, for the present optomechanical experiments, we did not use the electrostatic actuator to control the DC shuttles since the objective is to actuate the shuttle using the optical gradient force. For reference, we have included in Figure 6(b) the electrostatic MEMS-driven response of the DC shuttle around 720 kHz, corresponding to its fundamental mechanical resonance. We used an external photodetector (Thorlabs, DET01CFC) connected to a lock-in-amplifier (Zurich Instruments, HF2LI) to measure the frequency-dependent response of the electrostatic MEMS actuator.

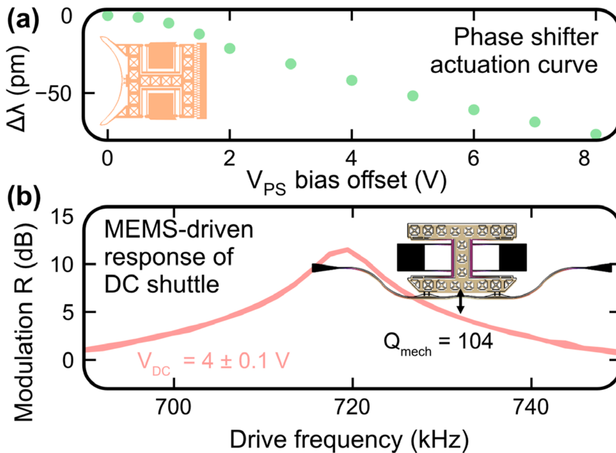

Figure 6: Electrostatic MEMS characterization of the phase shifter and the directional coupler. (a) Phase shifter response to a V_{PS} bias offset up to 8 V. (b) Frequency response measurement of the DC shuttle driven using an electrostatic MEMS comb-drive actuator.

Finally, we used the lock-in amplifier to demonstrate optomechanical coupling between the optical ring resonator cavity and the mechanical resonance of the DC shuttle at 720 kHz. We used two approaches for the demonstration: direct modulation of the laser power and electrostatic modulation of the resonance wavelength.

Laser output modulation

First, we demonstrated the optomechanical excitation of the in-plane fundamental mechanical resonance of the DC shuttles by modulating the output power of the laser. We used the lock-in-amplifier to modulate the laser source output by ±15 %. We swept the modulation frequency from 690 to 750 kHz and measured the change in output modulation at the through port for different laser wavelengths across the optical resonance (Figure 7(a)). For laser wavelengths outside of the optical resonance, the change in output modulation is zero since it only depends on the laser output modulation. For laser wavelengths within the optical resonance, the output modulation is either decreased (blue-detuned) or increased (red-detuned). We observed a non-zero output modulation for laser powers as low as 1 mW, see Figure 7(b).

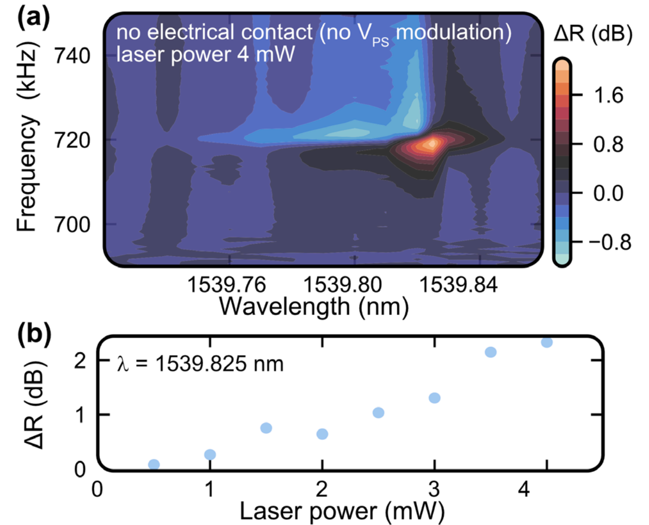

Figure 7: Optomechanical excitation of the suspended DC shuttle by laser power modulation. (a) Frequency response measurement repeated for different wavelengths across the optical resonance. (b) The effect could be observed with laser powers as low as 1 mW.

MEMS resonance modulation

We also demonstrated the optomechanical excitation of the same in-plane fundamental mechanical resonance of the directional coupler by driving the phase shifter in the ring electrostatically, see Figure 8. The output of the lock-in-amplifier was used to drive the phase shifter with an amplitude of 100 mV in the frequency range 690 to 750 kHz. We fixed the wavelength to 1539.82 nm, and repeated the frequency sweep for V_{PS} bias offsets up to 8 V.

Authorized licensed use limited to: IMEC. Downloaded on June 02,2024 at 13:25:49 UTC from IEEE Xplore. Restrictions apply.

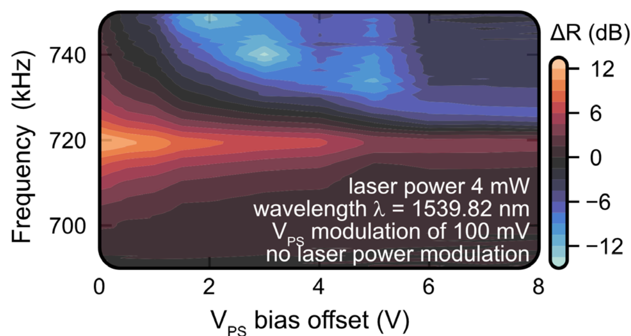

Figure 8: Optomechanical excitation of the suspended DC shuttle by round-trip phase modulation using the electrostatic MEMS actuator. Frequency response measurement repeated for different V_{PS} bias offsets.

CONCLUSION

We have demonstrated optomechanical coupling in a silicon photonic chip with local vacuum-sealing caps instead of using a traditional vacuum chamber. This new platform can open up the field of cavity optomechanics to new practitioners and promote its industrial growth for example in high precision sensors and quantum computing.

ACKNOWLEDGEMENTS

This work has received funding from the European Union's Horizon 2020 research and innovation programme under grant agreement No.780283 (MORPHIC). We thank Dr. Max Yan for access to measurement equipment.

CONTACT

*P. Edinger, edinger@kth.se

REFERENCES

[1] T. J. Kippenberg and K. J. Vahala, “Cavity Opto-Mechanics,” *Opt. Express*, vol. 15, no. 25, pp. 17172–17205, Dec. 2007, doi: 10.1364/OE.15.017172.

[2] M. Wang *et al.*, “Beating thermal noise in a dynamic signal measurement by a nanofabricated cavity optomechanical sensor,” *Sci. Adv.*, vol. 9, no. 11, p. eadf7595, Mar. 2023, doi: 10.1126/sciadv.adf7595.

[3] J. Roels, I. De Vlaminck, L. Lagae, B. Maes, D. Van Thourhout, and R. Baets, “Tunable optical forces between nanophotonic waveguides,” *Nat. Nanotechnol.*, vol. 4, no. 8, pp. 510–513, Aug. 2009, doi: 10.1038/nnano.2009.186.

[4] H. Cai *et al.*, “A nanoelectromechanical systems optical switch driven by optical gradient force,” *Appl. Phys. Lett.*, vol. 102, no. 2, p. 023103, Jan. 2013, doi: 10.1063/1.4775674.

[5] B. Dong *et al.*, “A silicon-nanowire memory driven by optical gradient force induced bistability,” *Appl. Phys. Lett.*, vol. 107, no. 26, p. 261111, Dec. 2015, doi: 10.1063/1.4939114.

[6] B. Dong *et al.*, “A nanoelectromechanical systems actuator driven and controlled by Q-factor attenuation of ring resonator,” *Appl. Phys. Lett.*, vol. 103, no. 18, p. 181105, Oct. 2013, doi: 10.1063/1.4827096.

[7] N. Quack *et al.*, “Integrated silicon photonic MEMS,” *Microsyst. Nanoeng.*, vol. 9, no. 1, Art. no. 1, Mar. 2023, doi: 10.1038/s41378-023-00498-z.

[8] M. W. Pruessner, D. Park, T. H. Stievater, D. A. Kozak, and W. S. Rabinovich, “Broadband opto-electro-mechanical effective refractive index tuning on a chip,” *Opt. Express*, vol. 24, no. 13, pp. 13917–13930, Jun. 2016, doi: 10.1364/OE.24.013917.

[9] P. Edinger *et al.*, “Vacuum-sealed silicon photonic MEMS tunable ring resonator with an independent control over coupling and phase,” *Opt. Express*, vol. 31, no. 4, pp. 6540–6551, Feb. 2023, doi: 10.1364/OE.480219.

[10] G. Jo *et al.*, “Wafer-level hermetically sealed silicon photonic MEMS,” *Photonics Res.*, vol. 10, no. 2, pp. A14–A21, Feb. 2022, doi: 10.1364/PRJ.441215.

Authorized licensed use limited to: IMEC. Downloaded on June 02,2024 at 13:25:49 UTC from IEEE Xplore. Restrictions apply.